Acta Crystallographica Section B
Structural Science
ISSN 0108-7681

Pressure-induced polymorphism in phenol

David R. Allan,[a]* Stewart J. Clark,[b] Alice Dawson,[c] Pamela A. McGregor[a] and Simon Parsons[c]

[a]School of Physics, The University of Edinburgh, Mayfield Road, Edinburgh EH9 3JZ, UK, [b]Department of Physics, Durham University, Science Laboratories, South Road, Durham DH1 3LE, UK, and [c]School of Chemistry, The University of Edinburgh, West Mains Road, Edinburgh EH9 3JJ, UK

Correspondence e-mail: dra@ph.ed.ac.uk

Received 20 March 2002
Accepted 11 October 2002

The high-pressure crystal structure of phenol (C_6H_5OH), including the positions of the H atoms, has been determined using a combination of single-crystal X-ray diffraction techniques and *ab initio* density-functional calculations. It is found that at a pressure of 0.16 GPa, which is just sufficient to cause crystallization of a sample held at a temperature just above its ambient-pressure melting point (313 K), a previously unobserved monoclinic structure with $P2_1$ symmetry is formed. The structure is characterized by the formation of hydrogen-bonded molecular chains, and the molecules within each chain adopt a coplanar arrangement so that they are ordered in an alternating 1-1-1 sequence. Although the crystal structure of the ambient-pressure $P112_1$ phase is also characterized by the formation of molecular chains, the molecules adopt an approximate threefold arrangement. A series of *ab initio* calculations indicates that the rearrangement of the molecules from helical to coplanar results in an energy difference of only 0.162 eV molecule^{-1} (15.6 kJ mole^{-1}) at 0.16 GPa. The calculations also indicate that there is a slight increase in the dipole moment of the molecules, but, as the high-pressure phase has longer hydrogen-bond distances, it is found that, on average, the hydrogen bonds in the ambient-pressure phase are stronger.

1. Introduction

Phenol (C_6H_5OH, monohydroxybenzene) is an economically important chemical reagent and is used in a wide variety of synthetic processes. It is a member of the monoalcohol series and, as its hydroxyl group is slightly acidic (pK_a at 298 K is 9.99 in aqueous solution), it is often referred to as carbolic acid. Below its melting point of 313 K, phenol crystallizes in a monoclinic structure with $P2_1$ symmetry (which is often reported in the non-conventional $P112_1$ setting) (Zavodnik *et al.*, 1987). The crystal structure is characterized by infinite hydrogen-bonded chains of molecules, which are aligned parallel to the crystallographic *b* axis of the unit cell, where the molecules are arranged in approximate threefold helices. This threefold helical arrangement is also observed in phase IV of tertiary-butanol [$(CH_3)_3COH$ (Steininger *et al.*, 1989)]. However, the other preceding members of the monoalcohol series that can crystallize rather than vitrify on cooling, methanol (CH_3OH; Torrie *et al.*, 1989; Boese, 2002), ethanol (CH_3CH_2OH; Jönsson, 1976) and cyclobutanol (C_4H_6OH; McGregor *et al.*, 2003), form structures that, although they are also characterized by infinite hydrogen-bonded chains, have molecular arrangements that are essentially planar. Steric effects dominate the adoption of either a helical or a planar conformation of the molecules along the hydrogen-bonded

Table 1
High-pressure data collection scan sequence for the Bruker APEX CCD diffractometer.

Run	2θ (°)	ω range (°)	φ (°)	Frames
1	−28.00	−8, −40	90.00	106
2	28.00	40, −40	90.00	266
3	−28.00	−140, −215	90.00	250
4	28.00	−140, −172	90.00	106
5	−28.00	−140, −218	270.00	260
6	28.00	−140, −172	270.00	106
7	−28.00	−8, −40	270.00	106
8	28.00	35, −40	270.00	250

chains; therefore, the relatively bulky R—OH tails in tertiary-butanol and phenol promote the formation of helical chains.

Intermolecular interactions, such as steric effects and hydrogen bonding, depend strongly on intermolecular distances; consequently, high pressure provides an excellent probe for the investigation of the structure and dynamics of molecular solids. A systematic study of molecular systems at high pressure is fruitful as competition between the various interactions causes phase transitions, including vitrification, as well as effecting crystal nucleation. Moreover, it is expected that this competition will lead to an alteration in the hierarchy of interaction strengths, and, for example, it has been proposed that with increasing pressure hydrogen bonding diminishes relative to repulsive forces (Angell, 1991; Cook *et al.*, 1992, 1994). In our previous high-pressure crystal structure studies of methanol (Allan *et al.*, 1998) and ethanol (Allan & Clark, 1999) we found that the molecular chains of both the high-pressure and the ambient-pressure phases are essentially flat and each crystalline phase is characterized by the sequence of parallel or antiparallel molecules along the chains. In Etter's graph-set notation (Bernstein *et al.*, 1995) these structures can all be designated as $C(2)$ (or variants thereof, depending on local symmetry conditions). However, this designation conveys little conformational information, and so in this analysis we have adopted an alternative formalism. For methanol, the high-pressure phase has a pair of molecules aligned parallel with one another and a third set antiparallel so that a 2-1-2-1 (two molecules parallel, one molecule antiparallel *etc.*) sequence is formed, while both of the ambient-pressure phases have an alternating 1-1-1 sequence of molecules (*i.e.* individual molecules are aligned antiparallel with one another in an alternating sequence). The ambient-pressure phase of ethanol has pairs of *trans* and *gauche* conformers linked in parallel so that these molecular pairs alternate in a 2-2-2 sequence along the chain. In the high-pressure structure the molecules are aligned in a very simple alternating 1-1-1 sequence, which is reminiscent of both of the ambient-pressure phases of methanol. For all of these phases, the molecules are small enough to be packed in a ribbon-like arrangement along the chains, and the variation of the steric effects with pressure only changes the parallel and antiparallel ordering of the molecules along the chains. Conversely, for phenol the steric factors between the comparatively large C_6H_5 groups are such that a ribbon-like arrangement of the molecules within the chains is no longer possible, and helical hydrogen-bonded chains of molecules are formed in the crystal structure under ambient conditions.

In this article, we report the high-pressure crystal structure of phenol, which has been obtained using single-crystal X-ray diffraction techniques. We find that the high-pressure structure shares the same monoclinic $P2_1$ symmetry as the ambient-pressure phase and is also characterized by the formation of infinite hydrogen-bonded molecular chains. However, the molecules within the chains of the high-pressure phase are coplanar and they adopt an alternating 1-1-1 sequence. Although the high-pressure structure is distinct from that of the ambient-pressure phase, a series of *ab initio* density-functional calculations indicates that the alteration of the arrangement of the molecules within the chains, from helical to ribbon-like, results in a relatively small reduction in the enthalpy (0.162 eV molecule^{-1} or 15.6 kJ mole^{-1}) for the high-pressure structure.

2. Experimental

2.1. Crystallography

The sample was prepared by heating crystalline phenol above its melting temperature of 313 K and then loading it, as a liquid, into a preheated Merrill–Bassett diamond-anvil cell (Merrill & Bassett, 1974) that had been equipped with 600 μm culet diamonds and a tungsten gasket. The sample was pressurized, while maintaining the cell's initial temperature, until the nucleation of several crystallites was observed. The temperature was then increased, so that the polycrystalline sample was partially remelted, and subsequently cycled close to this elevated melting temperature, in order to reduce the number of crystallites [in a manner similar to the method of Vos *et al.* (1992, 1993)]. Finally, on cooling to ambient temperature, at approximately 0.16 GPa, we obtained a single crystal that entirely filled the 200 μm gasket hole.

The diamond-anvil cell was mounted and centred on a Bruker SMART APEX diffractometer (graphite monochromated Mo $K\alpha$ radiation) and a sequence of eight data collection scans was initiated, as detailed in Table 1. The *SMART* program (Bruker, 2001) was used for data collection control, and, with a detector distance of 70 mm, 2θ was set at either +28° or −28° to provide maximum coverage while ensuring that the detector surface did not intercept the primary beam. (No beam stop is used, and with this selection of detector distance and 2θ the primary beam does not impinge on the detector aperture.) The eight scans were conducted as a sequence of frames that each had a range of 0.3° in ω and an exposure time of 30 s. The φ axis was fixed at either 90° or 270°, to ensure that the axis of the diamond-anvil cell was held parallel to the $\omega/2\theta$ plane so that absorption from the pressure-cell components was minimized and the maximum possible access of reciprocal space was achieved. As the APEX diffractometer has a three-circle goniometer the χ axis is permanently fixed at a value of 54.74°. The overall data collection time was 15 h. The sample reflections were identified by hand with the aid of the *SMART* code, and an orien-

Table 2
Experimental details.

Crystal data	
Chemical formula	C_6H_5OH
Chemical formula weight	94.11
Cell setting, space group	Monoclinic, $P2_1$
a, b, c (Å)	11.610 (4), 5.4416 (11), 12.217 (5)
β (°)	101.47 (3)
V (Å^3)	756.4 (4)
Z	6
D_x (Mg m^{-3})	1.240
Radiation type	Mo $K\alpha$
No. of reflections for cell parameters	331
θ range (°)	2.5–25.5
μ (mm^{-1})	0.083
Crystal form, colour	Cylindrical, colourless
Radius (mm)	0.1
Temperature (K)	293 (2)
Data collection	
Diffractometer	CCD area detector
Data collection method	ω scans
Absorption correction	*SADABS*
T_{min}	0.213
T_{max}	1.000
No. of measured, independent and observed parameters	1129, 455, 269
Criterion for observed reflections	$I > 2\sigma(I)$
R_{int}	0.0567
θ_{max} (°)	24.88
Range of h, k, l	$-12 \rightarrow h \rightarrow 12$ $-6 \rightarrow k \rightarrow 6$ $-7 \rightarrow l \rightarrow 7$
Refinement	
Refinement on	F^2
$R[F^2 > 2\sigma(F^2)]$, $wR(F^2)$, S	0.0863, 0.2777, 0.975
No. of reflections and parameters used in refinement	455, 29
H-atom treatment	Riding
Weighting scheme	$w = 1/[\sigma^2(F_o^2) + (0.1876P)^2]$ where $P = (F_o^2 + 2F_c^2)/3$
$(\Delta/\sigma)_{max}$	0.002
$\Delta\rho_{max}$, $\Delta\rho_{min}$ (e Å^{-3})	0.321, −0.199
No. of restraints	14

Computer programs used: *SMART* (Bruker, 2001), *SHELXTL* (Sheldrick, 1997), *SHELXS*97 (Sheldrick, 1990), *SHELXL*97 (Sheldrick, 1997).

tation matrix was determined using the *GEMINI* program (Sparks, 1999). Data integration and global-cell refinement were performed with the program *SAINT* (Bruker, 2001). The program *SHADE* (Allan *et al.*, 2000) was used to reject reflections for which either the incident or the diffracted beam was completely absorbed by the cell and resulted in the shading of the detector. Reflections with very poorly fitting profiles [*i.e.* those reflections with poor correlations (< 0.3) between their measured and calculated profiles] were also rejected. The surviving reflections were corrected for absorption by the pressure-cell components with the program *SADABS* (Sheldrick, 2001) and the transmission ranged from 0.494 to 1.000. The low minimum transmission factor arises because of partial shadowing by the highly absorbing tungsten gasket; this shadowing is difficult to model analytically.

One of the most serious difficulties encountered in high-pressure crystallography is the limited volume of reciprocal space that can be sampled because of shading by the body of the pressure cell. In molecular systems, where low-symmetry space groups are usual, data completeness may be only 20% or 30% depending on the orientation of the sample. The completeness of the data set collected here is only 20% to $2\theta = 50°$, and this lack of completeness presented difficulties during solution and refinement. The structure was solved in $P2_1$ using direct methods (*SHELXTL*; Sheldrick, 1997); two highly distorted phenol molecules were just recognizable from the initial maps. The third phenol molecule was located by iterative cycles of least-squares refinement (in which the phenyl rings were constrained to be perfect hexagons) and difference-Fourier syntheses. Solution recognition is difficult because Fourier peaks are broadened along directions that are related to poorly sampled regions of reciprocal space; Gilmore & Stewart (2001) have recently shown that map interpretation can be facilitated by the use of maximum entropy methods.

Owing to the poor completeness, a full anisotropic refinement with independent positional parameters for each atom was not possible. Instead the hexagon constraints on the phenyl rings were retained in the final model, while the geometries about the three independent hydroxyl moieties were restrained to be similar. A common overall isotropic displacement parameter was also refined. This model, which comprises 29 parameters and 14 restraints, converged to a conventional R factor ($R1$) of 8.63% (see Table 2). H atoms were placed in calculated positions, those related to O atoms being placed so as to optimize hydrogen bonding. An alternative model, in which the three phenol molecules were restrained to be geometrically similar and have C_{2v} symmetry, converged to $R1 = 7.67\%$ for 65 parameters and 104 restraints. We report the first of these models here since the Hamilton (1965) R-ratio test implies that this improvement in R factor is not statistically significant. A summary of the crystal, data collection and final refinement details are listed in Table 2. The refined fractional coordinates of the high-pressure structures are deposited.[1]

2.2. Theoretical calculations

Because the atomic positions are difficult to refine, we have also determined the full set of structural parameters for the various phases of phenol by performing a series of *ab initio* calculations using the *CASTEP* code (Payne *et al.*, 1992; Segall *et al.*, 2002). This has enabled us to obtain the positions of the H atoms that were only inferred from the data collected using the X-ray diffraction techniques.

The density-functional formalism was used to solve the electronic structure of the materials with the generalized gradient approximation (GGA) (Perdew & Wang, 1992) applied for the many-electron exchange and correlation interactions. GGAs are known to provide a very accurate description of the structural and electronic properties of hydrogen-bonded systems compared with the often-used local density approximation (Perdew & Zunger, 1981). Non-local ultrasoft pseudopotentials generated by the method of

[1] Supplementary data for this paper are available from the IUCr electronic archives (Reference: BM0050). Services for accessing these data are described at the back of the journal.

Vanderbilt (1990) are used to describe electron–ion interactions. The valence electron wavefunctions are expanded in a plane-wave basis set with a kinetic energy cut-off of 380 eV. This converges the total energy differences of the system to better than 0.001 eV molecule^{-1}. Brillouin zone integrations are performed on a Monkhorst–Pack (Monkhorst & Pack, 1976) grid that is taken large enough to reach a similar level of convergence in total energy as the wavefunction cut-off. The electronic structure calculation proceeds *via* a preconditioned conjugate gradients energy-minimization scheme (Perdew & Wang, 1992) and density-mixing algorithm using the plane-wave coefficients as variational parameters. We have also optimized the structural parameters, both internal coordinates and lattice parameters, using a conjugate-gradients scheme. We report the relaxed high-pressure and ambient-pressure structural parameters with the deposited experimental values. The lattice parameters from these calculations are found to be $a = 6.236$, $b = 9.071$, $c = 14.756$ Å, $\gamma = 90.136^\circ$ with $V = 834.70$ Å^3 for the ambient-pressure phase in the $P112_1$ setting and $a = 11.728$, $b = 5.560$, $c = 12.332$ Å, $\beta = 100.496^\circ$ with $V = 790.69$ Å^3 for the high-pressure phase in the $P12_11$ setting.

We have also performed a Mulliken population analysis on the systems, which has allowed us to examine the nature of the charge transfer between the various species in each of the structures. We have used the method described by Segall *et al.* (1996*a*,*b*) to calculate the Mulliken charges on the atoms. However, it is worth noting that several other methods exist, and the actual values of the charges change from method to method. Therefore, these values should not be taken as the actual atomic charge, which, in any case, is rather ambiguously defined. However, it is generally thought that the direction of charge transfer will be correct. The results of the analysis are illustrated in Fig. 1. We find that the charge distribution is fairly insensitive to the surroundings of the molecule, in that for the ambient-pressure and high-pressure structures considered here the atomic charges are relatively similar. However, we note that the most significant change is in the O—H bond and the C atom opposite, and this change indicates a slight increase in the strength of the hydrogen-bond within the high-pressure system compared with that in the ambient-pressure structure. We have used the distribution of atomic charges to calculate the dipole moment of the phenol molecule in each structure. We find that in the ambient-pressure structure there is a molecular dipole moment of 3.51 Debye, which increases slightly to 3.86 Debye in the high-pressure structure.

3. Discussion

The general features of packing motifs adopted by mono-alcohols, *R*OH, have been described by Brock & Duncan (1994). There is a conflict between the packing requirements of the *R* groups and the need to bring the small OH groups into close enough proximity to form a hydrogen bond. If the hydroxyl-containing molecules are relatively 'thin' (Brock's terminology) they can be related by a 2_1 screw axis or a glide plane. Steric hindrance between *R* groups prohibits this for bulkier molecules, and these systems often form helices about three-, four- or sixfold screw axes or contain more than one molecule in the asymmetric unit. To quote Brock directly: 'C_nH_mOH molecules with fully elaborated hydrogen-bond networks are much more likely to crystallize with $Z' > 1$ or in high-symmetry space groups than would be expected based on statistics determined for the Cambridge Structural Database as a whole'.

Viewed in this light the ambient- and high-pressure polymorphs of phenol exhibit quite typical packing motifs, with the phenyl group behaving as though it is 'borderline thin'. At ambient pressure, phenol behaves like a bulky molecule, with a structure with $Z' = 3$ that forms a pseudo-threefold helical chain (Fig. 2). The three molecules that compose the repeat-unit of the helix are not related to one another by symmetry, and it is only the neighbouring hydrogen-bonded chains that are related by a 2_1 screw axis. At 0.16 GPa, phenol behaves like a typical small alcohol (Fig. 3). The structure, which also has $Z' = 3$, consists of one crystallographically unique molecule that is disposed along a chain that is generated by a 2_1 axis (labelled '*C*' in the tables and supplemental data). A second very similar chain is built of two crystallographically independent molecules (labelled *A* and *B*). The molecules within each chain adopt a ribbon-like arrangement and they are ordered in an alternating 1-1-1 sequence.

When the high-pressure phase is viewed along the **c** direction, consecutive molecules in each chain appear to be arranged so that the phenyl groups adopt a herringbone arrangement (Fig. 4). The angles made between the planes of the phenol molecules labelled *A* and *B* and the plane containing the OH···OH hydrogen bonds are 36.9 (5)° and 31.6 (7)°, respectively; the angle between the planes of the *A* and *B* phenyl rings is 66.0 (3)°. The corresponding values for the molecule labelled 'C' are similar: 33.6 (8)° and 63.5 (4)°.

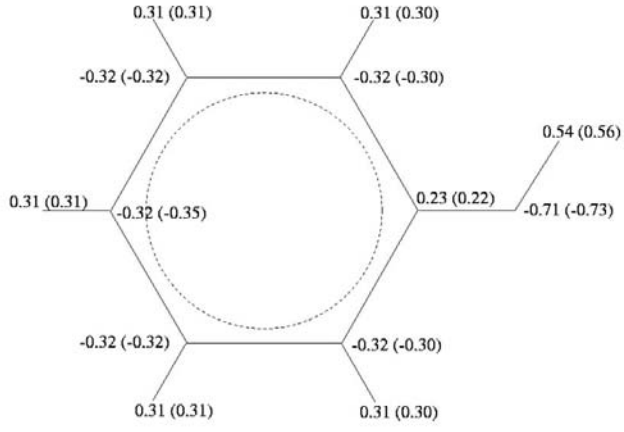

Figure 1
The results of the Mulliken analyses derived from plane-wave density-functional-theory calculations on the ambient- and high-pressure polymorphs of phenol. The numbers represent the nominal atomic charge in electrons and numbers given in parentheses are for the high-pressure phase.

This arrangement avoids close contacts between neighbouring CH groups along a chain.

As regards the packing of the chains, an analogy can be drawn between the high-pressure phase of phenol and the high-pressure, $P2_1/c$, structure of ethanol, in which alternating 1-1-1 molecular hydrogen-bonded chains of molecules are arranged so that they are coplanar and, consequently, layers of chains parallel to $(\bar{1}01)$ are produced. Within these layers, the chains are staggered so that the CH_3CH_2 tail groups interlock with one another. Analogously, for the high-pressure structure of phenol, layers of hydrogen-bonded chains are produced that are parallel to (100) and a very similar interlocking motif is adopted (Fig. 4). The layers appear to occupy the (300) planes, and the 300 reflection is the most intense in the data set. For ethanol, the rearrangement of the chains between the ambient-pressure and high-pressure phases is accompanied by a more efficient molecular packing: in the ambient-pressure structure, at 87 K, each molecule occupies a volume of 78.51 Å^3, while at high pressure the molecular volume is 75.99 Å^3. A comparable effect is also observed in phenol where each molecule occupies 131.33 Å^3 in the ambient-pressure structure while for the high-pressure phase there is an appreciable improvement in packing efficiency with each molecule occupying 126.07 Å^3.

In the ambient-pressure crystal structure the phenyl groups have a rather more complex interaction motif, though this motif is generally of the form expected from a herringbone arrangement. Neighbouring helical chains have two classes of phenyl contacts: the first comprises phenyl contacts where the axes of the molecules, as defined by the C—O vector, are arranged antiparallel to one another so that only pairs of molecules interact (*B* and *C*′); and in the second, the axes of the molecules (of type *A*) are directed towards the centre of the neighbouring chain so that they interact with a pair of molecules (type *B*′ and *C*′) on that adjacent chain (see Fig. 2).

It is interesting to note that the crystallographic screw axis is perpendicular to the axes of the helical chains themselves, and, consequently, the hydrogen bonding can be thought of as antiferroelectric in character: *i.e.* if we define the hydrogen bonds to be dipolar units, then the 2_1 screw axis ensures that half of the dipoles are arranged parallel to the *a* axis (along the length of the molecular chains) while half are arranged antiparallel. This means of describing a structure, while common in the physics literature, is rarely employed in chemistry. The

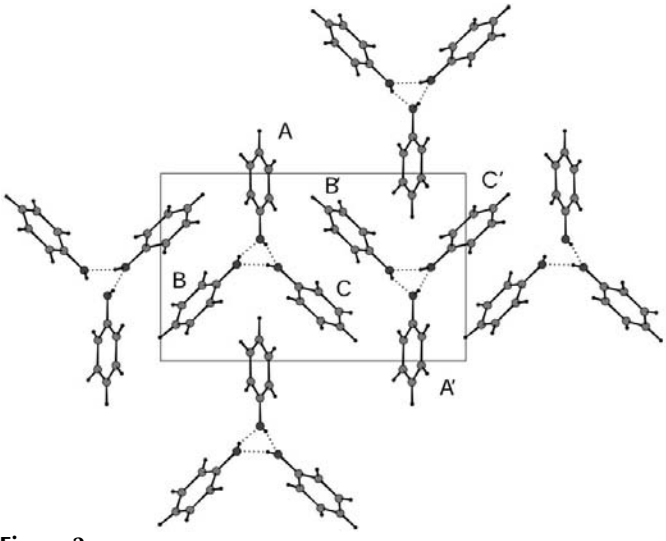

Figure 2
An *a* axis projection of the ambient-pressure, $P112_1$, structure of phenol, from Zavodnik *et al.* (1987). The crystallographic *b* axis is vertical while the *c* axis is horizontal. The helical hydrogen-bonded molecular chains are viewed along their lengths.

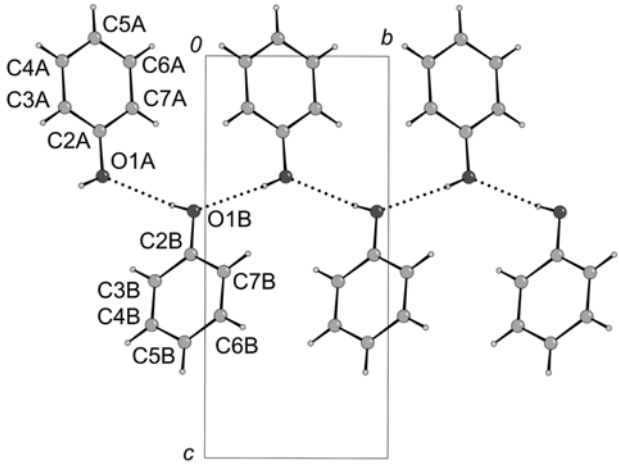

Figure 3
One of the crystallographically unique hydrogen-bonded chains in the high-pressure polymorph of phenol. The chain is viewed along the *a* axis. The molecules adopt an alternating 1-1-1 sequence.

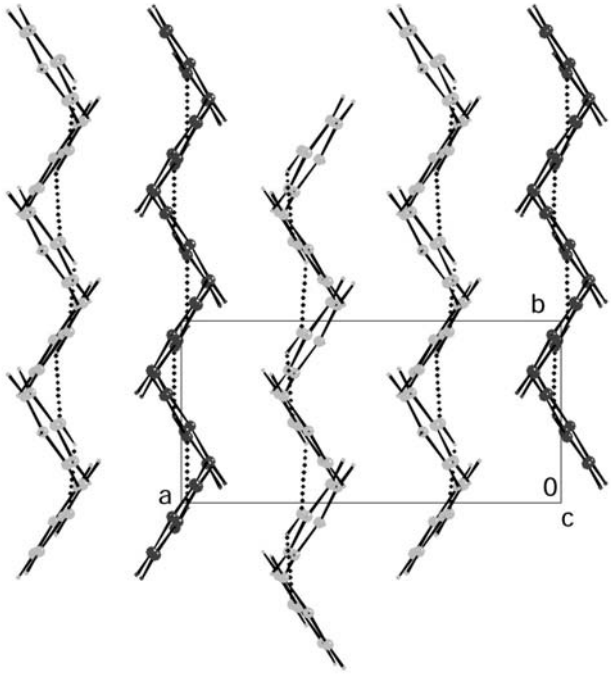

Figure 4
The high pressure phase of phenol viewed along the **c** direction. The chains generated by lattice repeat of the *A* and *B* molecules are shown in grey; the chains formed by the action of the 2_1 axis on the molecules labelled '*C*' are shown in black.

antiparallel arrangement of the hydrogen bonds does not necessarily mean that the ambient-pressure phase of phenol is antiferroelectric; a measurement of the dielectric properties would be required to establish antiferroelectricity. In the high-pressure phase both types of molecular chain are parallel to the polar 2_1 screw axis, and, consequently, the dipoles in the high-pressure phase have ferroelectric-like characteristics: *i.e.* the dipoles, as defined by the hydrogen bonds, can be arranged parallel to one another without altering the crystal symmetry – though it is possible for the H atoms in each chain type to order in a different sense with respect to the polar *b* axis (as is the case with the structure reported here).

In Table 3 we compare the experimental and *ab initio* bond lengths and bond angles for selected hydrogen bonds in both the high-pressure and the ambient-pressure structures. The values derived from the theoretical calculations are in good overall agreement with the values determined by experiment, although the experimental values tend to consistently underestimate the lengths of the bonds and generally give smaller O—H···O bond angles (*i.e.* hydrogen bonds that are less straight). The discrepancies are largest for dimensions that depend on the H-atom positions, which are difficult to determine accurately with X-ray diffraction techniques and have been treated during refinement with geometrical constraints. (For molecules closely related to phenol in the Cambridge Structural Database, O—H distances, as defined by internuclear separations, are generally found to be 1.000 Å, and this value gives a correction ratio of 1.217, on average, for the tabulated values of both the ambient-pressure and the high-pressure phases.) However, the distances that involve only the O atoms, which can be determined accurately both experimentally and theoretically, are in excellent agreement and differ by less than 2%. It is significant, though, that both the experimental and theoretical studies show that, on average, the O—O distances are 10% larger for the high-pressure structure than for the ambient-pressure phase.

We have also examined the hydrogen-bond strength in the ambient-pressure and high-pressure phases of phenol using a simple electrostatic model. We have used the charge-density analysis (Mulliken charges given in Fig. 1) and the hydrogen-bond distances to calculate values of Q_1Q_2/r (from Coulomb's law), which can be considered as a measure of the hydrogen-bond strength. Although the charge increases slightly on the O—H atoms in the high-pressure phase relative to the ambient-pressure phase, the H···O distances also increase. In addition, when we use this measure of the hydrogen-bond strength we find that the ambient-pressure hydrogen-bond strength is approximately 8% greater, on average, than that in the high-pressure phase. Despite the difference in hydrogen-bond strength we find that the two structures are energetically similar (they have an enthalpy difference of only 0.162 eV molecule^{-1} or 15.6 kJ mole^{-1}) at 0.16 GPa, and the energy is thus lowered in the high-pressure phase with an accompanying increase in packing efficiency.

The ambient-pressure structure has a pseudosymmetry with the orthorhombic $P222_1$ (Gillier-Pandraud, 1967) and $P2_122_1$ (Scheringer, 1963) space groups, and this is partly reflected in the small deviation of the monoclinic unit-cell axes from orthogonality ($\gamma = 90.360^\circ$). Indeed, the ambient-pressure crystal structure of phenol was originally identified as having $P222_1$ symmetry, although the same, and subsequent, workers established that the monoclinic $P112_1$ symmetry (an alternative setting of the conventional $P12_11$) is correct and allows for sensible hydrogen bonding. To test the stability of the $P112_1$ structure relative to either of the orthorhombic $P222_1$ or $P2_122_1$ symmetries we have performed calculations in which the symmetry of the ambient-pressure phase is reduced to $P1$ but the cell parameters and heavy-atom positions are taken from the $P222_1$ structure. Full structural relaxation results in a model that closely reproduces the ambient-pressure $P112_1$ phase and which has only a weak pseudosymmetry for either $P222_1$ or $P2_122_1$, at least for the C and O atoms. This result indicates that the $P112_1$ structure is the stable phase.

In conclusion, we have solved the high-pressure monoclinic, $P2_1$, crystal structure of phenol and find that at the modest pressure of 0.16 GPa a very different molecular-packing arrangement is adopted from that of the ambient-pressure phase. The high-pressure structure is characterized by hydrogen-bonded molecular chains that adopt an alternating 1-1-1 sequence, whereas the ambient-pressure phase is composed of chains where the molecules are arranged in approximate threefold helices. This rearrangement of the molecular chains not only offers a marked improvement in molecular packing efficiency for the overall crystal structure but also results in a small reduction of the calculated enthalpy.

Table 3
Selected hydrogen-bond lengths and bond angles for the high-pressure and ambient-pressure phases of phenol from the experimental studies and the *ab initio* calculations.

The experimental values for the ambient-pressure phase are taken from Zavodnik *et al.* (1987). We have denoted the acceptor and donor atoms that are involved in the bonds as *A* and *D*, respectively. Note that the *D*—H distances for the high-pressure refinement were restrained.

High-pressure phase

	D—H (Å)		H···*A* (Å)		<*DHA* (°)		*D*···*A* (Å)		
D—H	Expt.	Theor.	Expt.	Theor.	Expt.	Theor.	Expt.	Theor.	*A*
O1*A*—H1*A*	0.82	0.98	2.23	2.05	147.6	167.2	2.957	3.019	O1*B*
O1*B*—H1*B*	0.82	0.98	2.24	2.06	143.0	165.6	2.940	3.021	O1*A*
O1*C*—H1*C*	0.82	0.98	2.26	2.07	148.8	166.9	2.996	3.035	O1*C*

Ambient-pressure phase (Zavodnik *et al.*, 1987)

	D—H (Å)		H···*A* (Å)		<*DHA* (°)		*D*···*A* (Å)		
D—H	Expt.	Theor.	Expt.	Theor.	Expt.	Theor.	Expt.	Theor.	*A*
O1*A*—H1*A*	0.74	1.00	1.98	1.76	164.7	174.3	2.693	2.757	O1*C*
O1*B*—H1*B*	0.82	1.00	1.89	1.67	156.0	177.1	2.655	2.673	O1*A*
O1*C*—H1*C*	0.91	1.00	1.81	1.70	157.2	167.2	2.664	2.687	O1*B*

We would like to express our thanks to Dr J. S. Loveday and Professor R. J. Nelmes for a number of fruitful discussions. This work is supported by a grant from the Engineering and Physical Sciences Research Council (EPSRC) of the United Kingdom. The EPSRC also funds the PhD studentships for PAM and AD, and an EPSRC Advanced Fellowship currently

supports DRA. *CASTEP* version 4.2 is licensed under the UKCP/MSI agreement.

References

Allan, D. R. & Clark, S. J. (1999). *Phys. Rev. B*, **60**, 6328–6334.
Allan, D. R., Clark, S. J., Brugmans, M. J. P., Ackland, G. J. & Vos, W. L. (1998). *Phys. Rev. B*, **58**, R11809–R11812.
Allan, D. R., Clark, S. J., Parsons, S. & Ruf, M. (2000). *J. Phys. Condens. Matter*, **12**, L613–L618.
Angell, C. A. (1991). *J. Non-Cryst. Solids*, **13**, 133.
Bernstein, J., Davis, R. E., Shimoni, L. & Chang, N-L. (1995). *Angew. Chem. Int. Ed. Engl.* **34**, 1555–1573.
Boese, R. (2002). Private communication.
Brock, C. P. & Duncan, L. L. (1994). *Chem. Mater.* **6**, 1307–1312.
Bruker (2001). *SMART Data Collection and SAINT Integration Programs for Area Detector Data.* Bruker AXS, Madison, Wisconsin, USA.
Cook, R. L., King H. E., Herbst, C. A. & Herschbach, D. R. (1994). *J. Chem. Phys.* **100**, 5178–5189.
Cook, R. L., King, H. E. & Pfeiffer, D. G. (1992). *Phys. Rev. Lett.* **69**, 3072–3075.
Gillier-Pandraud, H. (1967). *Bull. Soc. Chim. Fr.* **6**, 1988.
Gilmore, C. J. (2001). Plenary lecture delivered at the European Crystallography Meeting ECM20, Krakow, Poland, 25–31 August 2001.
Gilmore, C. J. & Stewart, A. (2001). Personal communication.
Hamilton, W. L. (1965). *Acta Cryst.* **18**, 502–510.
Jönsson, P. G. (1976). *Acta Cryst.* B**32**, 232–235.
McGregor, P. A., Allan, D. R., Clark, S. J. & Parsons, S. (2003). In preparation.
Merrill, L. & Bassett, W. A. (1974). *Rev. Sci. Instrum.* **45**, 290–294.
Monkhorst, H. J. & Pack, J. D. (1976). *Phys. Rev. B*, **13**, 5188.
Payne, M. C., Teter, M. P., Allan, D. C., Arias, T. A. & Joannopolous, J. D. (1992). *Rev. Mod. Phys.* **64**, 1045–1097.
Perdew, J. P. & Wang, Y. (1992). *Phys. Rev. B*, **45**, 13244–13249.
Perdew, J. P. & Zunger, A. (1981). *Phys. Rev. B*, **23**, 5048–5079.
Scheringer, C. (1963). *Z. Kristallogr.* **119**, 273.
Segall, M. D., Lindan, P. L. D., Probert, M. J., Pickard, C. J., Hasnip, P. J., Clark, S. J. & Payne, M. C. (2002). *J. Phys. Condens. Matter*, **14**, 2717–2744.
Segall, M. D., Shah, R., Pickard, C. J. & Payne, M. C. (1996*a*). *Phys. Rev. B*, **54**, 16317–16320.
Segall, M. D., Shah, R., Pickard, C. J. & Payne, M. C. (1996*b*). *Mol. Phys.* **89**, 571–577.
Sheldrick, G. M. (1990). *Acta Cryst.* A**46**, 467–473.
Sheldrick, G. M. (1997). *SHELXTL. SHELXL*97. University of Göttingen, Germany, and Bruker AXS, Madison, Wisconsin, USA.
Sheldrick, G. M. (2001). *SADABS.* University of Göttingen, Germany, and Bruker AXS, Madison, Wisconsin, USA.
Sparks, R. A. (1999). *GEMINI.* Bruker AXS, Madison, Wisconsin, USA.
Steininger, R., Bilgram, J. H., Gramlich, V. & Petter, W. (1989). *Z. Kristallogr.* **187**, 1–13.
Torrie, B. H., Weng, S.-X. & Powell, B. M. (1989). *Mol. Phys.* **67**, 575–581.
Vanderbilt, D. (1990). *Phys. Rev. B*, **41**, 7892–7995.
Vos, W. L., Finger, L. W. & Hemley, R. J. (1992). *Nature* (*London*), **358**, 46–48.
Vos, W. L., Finger, L. W. & Hemley, R. J. (1993). *Phys. Rev. Lett.* **71**, 3150–3153.
Zavodnik, V. E., Bel'skii, V. K. & Zorkii, P. M. (1987). *Zh. Strukt. Khim.* **28**, 175.